Phase-sensitive manipulations of the two-mode entangled state by a type-II nondegenerate optical parametric amplifier inside an optical cavity

Haixia Chen and Jing Zhang*

State Key Laboratory of Quantum Optics and Quantum Optics Devices, Institute of Opto-Electronics, Shanxi University, Taiyuan 030006, People's Republic of China

(Received 6 March 2009; published 18 June 2009)

The quantum fluctuations and correlations of the output signal and idler beams from a type-II polarization nondegenerate optical parametric amplifier (NOPA) inside an optical cavity are investigated theoretically, which is driven by the different kinds of quantized fields such as the two-mode thermal field, the phase-conjugate state, and a pair of EPR beams at the signal and idler frequency. Spectral line shapes due to quantum interferences between the input quantum fields and the generated down-converted subharmonic fields of NOPA are studied by scanning the length of the NOPA cavity. The entanglement degree of the EPR entangled beams injected into the NOPA as signal and idler beams can be increased or decreased, which are realized by controlling the relative phase between the pump beam and the injected beams for the NOPA. The results demonstrate coherent phenomena of NOPA in the quantum regime and show phase-sensitive manipulations of quantum entanglement for quantum information processing.

DOI: 10.1103/PhysRevA.79.063826 PACS number(s): 42.50.Lc, 42.50.St, 42.65.Lm, 42.65.Yj

I. INTRODUCTION

It is well known that the parametric interactions generate optical fields which have important quantum properties. There have been much recent interests in the quantum features displayed in the output fields of the parametric process. The two-mode quadrature squeezed state of light and the quantum correlated twin beams have been generated directly from continuous type-II nondegenerate optical parametric oscillators (NOPO) operated below and above the oscillation threshold, respectively [1,2]. Some quantum information protocols such as quantum dense coding [3], unconditional entanglement swapping [4], have been realized by employing the type-II nondegenerate optical parametric amplifier (NOPA). The parametric process inside a cavity is a very efficient method to generate quantum optical field and becomes very fruitful in continuous-variable (CV) quantum communication and information. Another important aspect is the manipulating quantum states of light through the optical parametric amplifier (OPA), which is important for the quantum information propagation and communication. An OPA can be used to amplify nonclassical states such as squeezed states and single-photon states. This process is proved to be essential in the implementations of discrete-variable and CV quantum information processing, such as optimal quantum cloning machines [5], quantum nondemolition measurements [6], and CV all-optical quantum teleportation [7].

Recently, a series of phenomena on the interference in the type-I OPA inside an optical cavity has been studied experimentally with the injection of the coherent signal beam [8,9]. Later, Agarwal [10] generalized the observation of classical interference phenomena in the type-I OPA system injected with the coherent signal beam [8] to the quantum domain and studied theoretically the interferences of the quantum fluctuations from a type-I OPA when the cavity is driven by a quantized field. Recently, such quantum interference phenomenon was demonstrated experimentally in the phase-sensitive type-I OPA system inside an optical cavity with an injected squeezed vacuum state [11].

In this paper, we theoretically investigate the quantum fluctuations and correlations of the output signal and idler beams from a type-II polarization nondegenerate OPA inside an optical cavity, which is driven by the different kinds of quantized fields such as the two-mode thermal field, the phase-conjugate state, and a pair of EPR beams at the signal and idler frequency. Spectral line shapes due to quantum interferences between the input quantum fields and the generated down-converted subharmonic fields are studied by scanning the length of the NOPA cavity. We show how the quantum fluctuations and correlations of the input states can be modified and controlled by the NOPA inside an optical cavity. Especially, we demonstrate the degree of the correlation of input entangled beams can be improved by the proper choice of the relative phase between the pump field and the injected fields. This scheme can be straightforwardly implemented with a setup that is at present experimentally accessible.

This paper is arranged as follows. In Sec. II we present how the NOPA without the cavity phase sensitively manipulates the different kinds of the input two-mode states. In Sec. III the quantum fluctuations and correlations spectra of the output signal and idler beams from a NOPA inside an optical cavity are studied by scanning the length of the cavity. These results demonstrate that the NOPA inside a cavity can give the new phenomenon and present the novel spectral line shapes, which are caused by the interference between the harmonic pump field and the subharmonic seed field in NOPA in cooperation with the absorptive and dispersive responses of an optical cavity. A brief summary of the paper is presented in Sec. IV.

*Corresponding author; jzhang74@yahoo.com; jzhang74@sxu.edu.cn

II. PHASE-SENSITIVE MANIPULATION OF QUANTUM CORRELATIONS AND ENTANGLEMENT BY NOPA

First, we consider the simple NOPA process without considering cavity to investigate the quantum fluctuations and correlations with different kinds of quantized input fields. The quantum states we consider in this paper are described with the electromagnetic field annihilation operator $\hat{a}=(\hat{X}+i\hat{Y})/2$, which is expressed in terms of the amplitude $\hat{X}$ and phase $\hat{Y}$ quadrature with the canonical commutation relation $[\hat{X},\hat{Y}]=2i$. The phase-sensitive type-II polarization nondegenerate parametric amplifier can be expressed by the simple interaction Hamiltonian

$$H_I = i\hbar\kappa[e^{i\theta_p}\hat{a}_1^\dagger\hat{a}_2^\dagger - e^{-i\theta_p}\hat{a}_1\hat{a}_2]. \tag{1}$$

Here, $\hat{a}_1$ and $\hat{a}_2$ are the annihilation operators of the signal and idler fields of the NOPA, which have the frequency $\omega_s+\omega_i=\omega_p$ with orthogonal polarization. $\kappa=g\beta$ is a nonlinear coupling coefficient proportional to the nonlinear susceptibility g of the medium and to the amplitude β of the pump field. θ_p is the phase of the pump field relative to signal field (here the idler field has the same phase with the signal field without the loss of generality). Note that we assume that the nonlinear medium is pumped with the second-harmonic wave of ω_p and the pump field is undepleted and of sufficient intensity that it may be modeled classically. From Eq. (1), the creation and annihilation operators of the output modes of the NOPA after an interaction time T with the medium can be given by

$$\hat{a}_1^o = \hat{a}_1^{in}\cosh r + \hat{a}_2^{\dagger in}e^{i\theta_p}\sinh r,$$

$$\hat{a}_2^o = \hat{a}_2^{in}\cosh r + \hat{a}_1^{\dagger in}e^{i\theta_p}\sinh r, \tag{2}$$

where $r=\kappa T$ and $\hat{a}_1^{in}$ and $\hat{a}_2^{in}$ are the annihilation operators of the signal and idler input fields of the NOPA. The quadrature phase amplitudes of the output modes of the NOPA can be expressed by

$$\hat{X}_1^o = \hat{X}_1^{in}\cosh r + \hat{X}_2^{in\theta_p}\sinh r,$$

$$\hat{Y}_1^o = \hat{Y}_1^{in}\cosh r - \hat{Y}_2^{in\theta_p}\sinh r,$$

$$\hat{X}_2^o = \hat{X}_2^{in}\cosh r + \hat{X}_1^{in\theta_p}\sinh r,$$

$$\hat{Y}_2^o = \hat{Y}_2^{in}\cosh r - \hat{Y}_1^{in\theta_p}\sinh r. \tag{3}$$

Here, $\hat{X}_i^{\theta_p}=\hat{a}_i e^{-i\theta_p}+\hat{a}_i^\dagger e^{i\theta_p}$ and $\hat{Y}_i^{\theta_p}=-i(\hat{a}_i e^{-i\theta_p}-\hat{a}_i^\dagger e^{i\theta_p})$. To measure the degree of correlation between the two modes, we consider the variance $v(\theta,\varphi)=\langle\delta^2(X_1^\theta-X_2^\varphi)\rangle$. If $v(\theta,\varphi)=0$, then X_1^θ is perfectly correlated with X_2^φ. This means a measurement of X_1^θ can be used to infer a value of X_2^φ with certainty. Of course, X_1^θ and X_2^φ are uncorrelated when $v(\theta,\varphi)\geq 2$. The nonseparability criterion in terms of measurable squeezing variances of two-mode states

$$\langle\delta^2(\hat{X}_1^o \pm \hat{X}_2^o)\rangle + \langle\delta^2(\hat{Y}_1^o \mp \hat{Y}_2^o)\rangle < 4. \tag{4}$$

This is a sufficient criterion for nonseparability for any two-mode entangled state, which puts in the form suitable for experimental verification [12,13]. This inequality can be tested by the method called local measurement for the entanglement, for example, with a single polarized beam splitter. The polarized beam splitter provides the suitable quadrature combinations of the signal and idler fields for amplitude and phase quadrature simultaneously detectable at the two output ports. However, instead of simultaneous detection of the relevant quadrature combinations (local measurement), another method, called nonlocal measurement, can check the inequality. The signal and idler fields may be sent to two remote stations, respectively, then detected by two homodyne detections. It requires switching the two local oscillator phases from amplitude to phase quadrature measurements. This sequence of detections requires preparing an ensemble of identical states.

From the Eq. (3), the difference and the sum of the amplitude phase quadratures of the output modes of NOPA can be obtained

$$\hat{X}_1^o - \hat{X}_2^o = (\hat{X}_1^{in} - \hat{X}_2^{in})e^{-(+)r},$$

$$\hat{Y}_1^o + \hat{Y}_2^o = (\hat{Y}_1^{in} + \hat{Y}_2^{in})e^{-(+)r},$$

$$\hat{X}_1^o + \hat{X}_2^o = (\hat{X}_1^{in} + \hat{X}_2^{in})e^{+(-)r},$$

$$\hat{Y}_1^o - \hat{Y}_2^o = (\hat{Y}_1^{in} - \hat{Y}_2^{in})e^{+(-)r}, \tag{5}$$

where the minus and plus symbols outside or inside round brackets at exponent correspond to NOPA operated at amplification ($\theta_p=0$) or deamplification ($\theta_p=\pi$), respectively. When $\theta_p=0$, the NOPA is operated at the parametric amplification in which the injected subharmonic signal and harmonic pump fields are in phase. When the injected subharmonic signal and harmonic pump fields are out of phase, i.e., $\theta_p=\pi$, the NOPA is operated at the parametric deamplification.

Case 1. Consider the vacuum states as the signal and idler input fields with $\langle\delta^2\hat{X}_1^{in}\rangle=\langle\delta^2\hat{X}_2^{in}\rangle=\langle\delta^2\hat{Y}_1^{in}\rangle=\langle\delta^2\hat{Y}_2^{in}\rangle=1$. When the NOPA is operated at parametric amplification, the variances of the signal and idler output fields are expressed by

$$\langle\delta^2\hat{X}_1^o\rangle = \langle\delta^2\hat{X}_2^o\rangle = \langle\delta^2\hat{Y}_1^o\rangle = \langle\delta^2\hat{Y}_2^o\rangle = \frac{e^{-2r}+e^{2r}}{2} \tag{6}$$

and the correlated variances are given by

$$\langle\delta^2(\hat{X}_1^o - \hat{X}_2^o)\rangle = \langle\delta^2(\hat{Y}_1^o + \hat{Y}_2^o)\rangle = 2e^{-2r}$$

$$\langle\delta^2(\hat{X}_1^o + \hat{X}_2^o)\rangle = \langle\delta^2(\hat{Y}_1^o - \hat{Y}_2^o)\rangle = 2e^{2r}. \tag{7}$$

In the limit of $r\to\infty$, the perfect correlation with quadrature amplitude correlation and quadrature phase anticorrelation is achieved and each beam of the signal and idler output fields has infinite energy. When the NOPA is operated at the parametric deamplification, i.e., $\theta_p=\pi$, the two output modes are

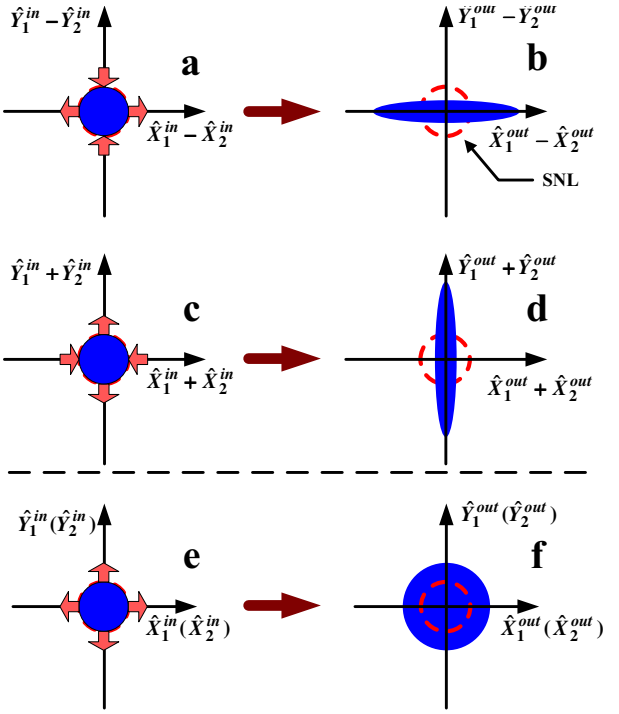

FIG. 1. (Color online) Schematics of the correlation and the quadrature components of the signal and idler output fields in the phase space with the input vacuum states for a NOPA. (a) and (c) are the quantum correlations of the input signal and idler fields; (b) and (d) are the quantum correlations of the output signal and idler fields; (e) and (f) are the input and output quadrature components of the signal and idler fields.

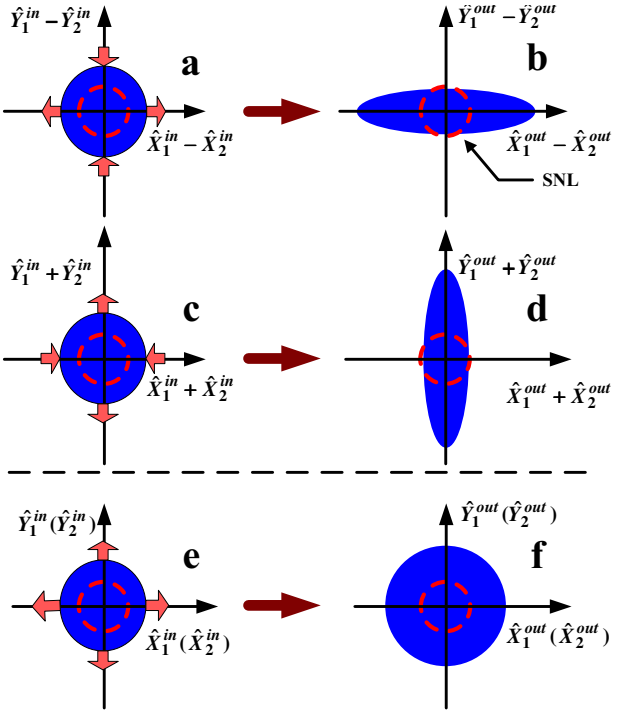

FIG. 2. (Color online) Schematics of the correlation and the quadrature components of the signal and idler output fields in the phase space with two input uncorrelated thermal optical fields for a NOPA. (a) and (c) are the quantum correlations of the input signal and idler fields; (b) and (d) are the quantum correlations of the output signal and idler fields; (e) and (f) are the input and output quadrature components of the signal and idler fields.

EPR entangled beams with quadrature amplitude anticorrelation and quadrature phase correlation

$$\langle \delta^2(\hat{X}_1^o + \hat{X}_2^o)\rangle = \langle \delta^2(\hat{Y}_1^o - \hat{Y}_2^o)\rangle = 2e^{-2r},$$

$$\langle \delta^2(\hat{X}_1^o - \hat{X}_2^o)\rangle = \langle \delta^2(\hat{Y}_1^o + \hat{Y}_2^o)\rangle = 2e^{2r}. \quad (8)$$

This case is a usual way to generate EPR entangled beams [1]. Since the signal and idler input fields are the vacuum states which are isotropic in phase space, the output fields of the NOPA have the same entangled degree, which is independent of the relative phase with the pump light. By selecting the proper phases of local oscillators, we can achieve the same entanglement. Figure 1 shows the schematic of the correlation and the quadrature components of the signal and idler output fields in the phase space by injecting the input vacuum states into the NOPA.

Case 2. Consider the two uncorrelated thermal optical fields as the input signal and idler modes with $\langle \delta^2 \hat{X}_1^{in}\rangle = \langle \delta^2 \hat{X}_2^{in}\rangle = \langle \delta^2 \hat{Y}_1^{in}\rangle = \langle \delta^2 \hat{Y}_2^{in}\rangle = e^{2r_0}$. When the NOPA is operated at parametric amplification, the variances of the signal and idler output fields are expressed by

$$\langle \delta^2 \hat{X}_1^o\rangle = \langle \delta^2 \hat{X}_2^o\rangle = \langle \delta^2 \hat{Y}_1^o\rangle = \langle \delta^2 \hat{Y}_2^o\rangle = \frac{e^{-2r} + e^{2r}}{2} e^{2r_0} \quad (9)$$

and the correlated variances are given by

$$\langle \delta^2(\hat{X}_1^o - \hat{X}_2^o)\rangle = \langle \delta^2(\hat{Y}_1^o + \hat{Y}_2^o)\rangle = 2e^{2(-r+r_0)},$$

$$\langle \delta^2(\hat{X}_1^o + \hat{X}_2^o)\rangle = \langle \delta^2(\hat{Y}_1^o - \hat{Y}_2^o)\rangle = 2e^{2(r+r_0)}. \quad (10)$$

When the NOPA is operated at parametric deamplification, the quantum correlation variances between the output modes can be expressed by

$$\langle \delta^2(\hat{X}_1^o + \hat{X}_2^o)\rangle = \langle \delta^2(\hat{Y}_1^o - \hat{Y}_2^o)\rangle = 2e^{2(-r+r_0)},$$

$$\langle \delta^2(\hat{X}_1^o - \hat{X}_2^o)\rangle = \langle \delta^2(\hat{Y}_1^o + \hat{Y}_2^o)\rangle = 2e^{2(r+r_0)}. \quad (11)$$

The output fields of the NOPA with the two uncorrelated thermal input fields are similar as the input vacuum states, which are also independent of the relative phase with the pump light. The schematic of the correlation and the quadrature components of the signal and idler output fields in the phase space with the injection of the input uncorrelated thermal optical fields into the NOPA is shown in Fig. 2.

Case 3. Consider the phase-conjugate states $|\hat{a}_1^{in}\rangle = |\frac{1}{2}(x+ip)\rangle$ and $|\hat{a}_2^{in}\rangle = |\frac{1}{2}(x-ip)\rangle$ as the input signal and idler modes injected into the NOPA. The variances of the signal and idler input fields are expressed by

$$\langle \delta^2 \hat{X}_1^{in}\rangle = \langle \delta^2 \hat{X}_2^{in}\rangle = \langle \delta^2 \hat{Y}_1^{in}\rangle = \langle \delta^2 \hat{Y}_2^{in}\rangle = e^{2r_0},$$

and the correlated variances are given by

$$\langle \delta^2(\hat{X}_1^{in} - \hat{X}_2^{in})\rangle = \langle \delta^2(\hat{Y}_1^{in} + \hat{Y}_2^{in})\rangle = 2,$$

$$\langle \delta^2(\hat{X}_1^{in} + \hat{X}_2^{in})\rangle = \langle \delta^2(\hat{Y}_1^{in} - \hat{Y}_2^{in})\rangle = 4e^{2r_0} - 2. \quad (12)$$

It is has been shown that a pair of phase-conjugate states carries more information than a pair of identical coherent states [14]. This property enables one to achieve better fidelities with a cloning machine admitting phase-conjugate input coherent states compared to the conventional case with identical input copies. Based on the above properties, Cerf and Iblisdir derived a CV cloning transformation [15] that uses N copies of a coherent state and N' copies of its complex conjugate as input states and produces M optimal clones of the coherent state and $M'=M+N'-N$ phase-conjugate clones (anticlones or time-reversed states). A much simpler and efficient CV phase-conjugate input (PCI) cloning machine based on linear optics, homodyne detection, and feed forward was proposed [16,17] and implemented experimentally [17]. In fact, the phase-conjugate coherent states are an ensemble of quasiclassical states which are neither squeezed nor entangled and nevertheless show some kind of nonlocality [18]. For the NOPA operated at the state of amplification, the variances of the signal and idler output fields are expressed by

$$\langle \delta^2 \hat{X}_1^o\rangle = \langle \delta^2 \hat{X}_2^o\rangle = \langle \delta^2 \hat{Y}_1^o\rangle = \langle \delta^2 \hat{Y}_2^o\rangle = \frac{e^{2r}}{2}(2e^{2r_0} - 1) + \frac{e^{-2r}}{2} \quad (13)$$

and the quantum correlation correlated variances are given by

$$\langle \delta^2(\hat{X}_1^o - \hat{X}_2^o)\rangle = \langle \delta^2(\hat{Y}_1^o + \hat{Y}_2^o)\rangle = 2e^{-2r},$$

$$\langle \delta^2(\hat{X}_1^o + \hat{X}_2^o)\rangle = \langle \delta^2(\hat{Y}_1^o - \hat{Y}_2^o)\rangle = (4e^{2r_0} - 2)e^{2r}. \quad (14)$$

The schematic of the correlation and the quadrature components of the signal and idler fields in the phase space with a pair of phase-conjugate input states for the NOPA operated at the state of amplification is shown in Fig. 3. We find the output signal and idler fields in Eq. (14) always satisfy the criterion of nonseparability when the NOPA is operated at the state of amplification with $r>0$. However they are not the minimum uncertainty states as shown in Fig. 3. The variances of the signal (or idler) output fields always increase with the increase of the parametric gain.

When the NOPA is operated at the state of deamplification, the variances of the signal and idler output fields are expressed by

$$\langle \delta^2 \hat{X}_1^o\rangle = \langle \delta^2 \hat{X}_2^o\rangle = \langle \delta^2 \hat{Y}_1^o\rangle = \langle \delta^2 \hat{Y}_2^o\rangle = \frac{e^{2r}}{2} + \frac{e^{-2r}}{2}(2e^{2r_0} - 1) \quad (15)$$

and the quantum correlation correlated variances are given by

$$\langle \delta^2(\hat{X}_1^o - \hat{X}_2^o)\rangle = \langle \delta^2(\hat{Y}_1^o + \hat{Y}_2^o)\rangle = 2e^{2r},$$

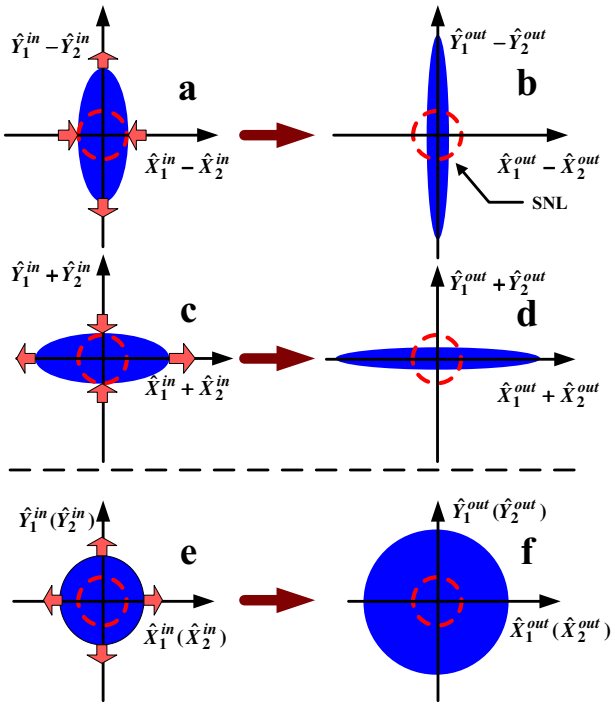

FIG. 3. (Color online) Schematics of the correlation and the quadrature components of the signal and idler fields in the phase space with a pair of phase-conjugate input states for the NOPA operated at the state of amplification. (a) and (c) are the quantum correlations of the input signal and idler fields; (b) and (d) are the quantum correlations of the output signal and idler fields; (e) and (f) are the input and output quadrature components of the signal and idler fields.

$$\langle \delta^2(\hat{X}_1^o + \hat{X}_2^o)\rangle = \langle \delta^2(\hat{Y}_1^o - \hat{Y}_2^o)\rangle = (4e^{2r_0} - 2)e^{-2r}. \quad (16)$$

The schematics of the correlation and the quadrature components of the signal and idler fields in the phase space with a pair of phase-conjugate input states for the NOPA operated at the state of deamplification are shown in Fig. 4. The variances of the signal (or idler) output fields will first decrease to reach the minimum value $(\langle \delta^2 \hat{X}_1^o\rangle_{\min} = \langle \delta^2 \hat{X}_2^o\rangle_{\min} = \langle \delta^2 \hat{Y}_1^o\rangle_{\min} = \langle \delta^2 \hat{Y}_2^o\rangle_{\min} = \sqrt{2e^{2r_0} - 1})$ then increase with the increase of the parametric gain. Comparing Eqs. (14) to Eqs. (16), we know that the output fields of the NOPA will have a different degree of the entanglement at the same parametric gain, which depends on the relative phase with the pump light due to the anisotropic property of the input fields in phase space for the phase-conjugate states as shown in Figs. 3 and 4.

Case 4. Consider an EPR entangled beam as the input signal and idler modes of NOPA, which have the quantum correlation, i.e., both their difference-amplitude quadrature variance $\langle \delta^2(\hat{X}_1^{in} - \hat{X}_2^{in})\rangle = 2e^{-2r_0}$ and sum-phase quadrature variance $\langle \delta^2(\hat{Y}_1^{in} + \hat{Y}_2^{in})\rangle = 2e^{-2r_0}$, are less than the quantum noise limit, where r_0 is squeezing factor. The output modes of the NOPA operated at parametric amplification are given by

$$\langle \delta^2 \hat{X}_1^o\rangle = \langle \delta^2 \hat{X}_2^o\rangle = \langle \delta^2 \hat{Y}_1^o\rangle = \langle \delta^2 \hat{Y}_2^o\rangle = \frac{e^{-2(r+r_0)} + e^{2(r+r_0)}}{2},$$

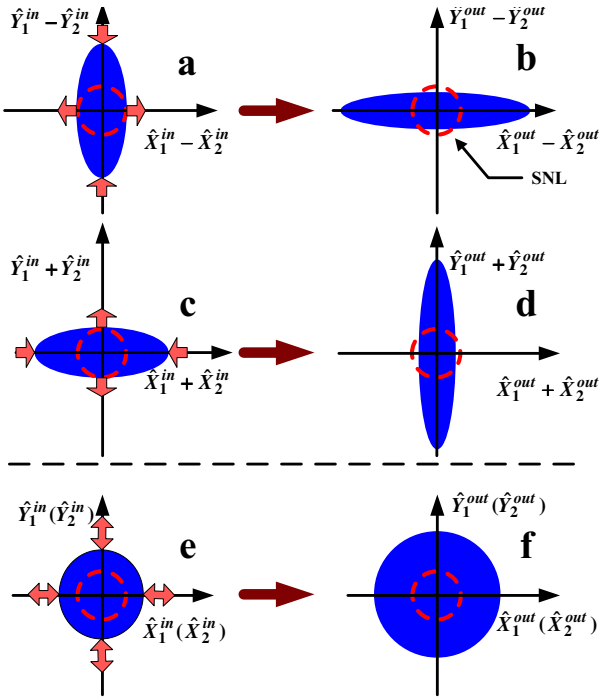

FIG. 4. (Color online) Schematics of the correlation and the quadrature components of the signal and idler fields in the phase space with a pair of phase-conjugate input states for the NOPA operated at the state of deamplification. (a) and (c) are the quantum correlations of the input signal and idler fields; (b) and (d) are the quantum correlations of the output signal and idler fields; (e) and (f) are the input and output quadrature components of the signal and idler fields.

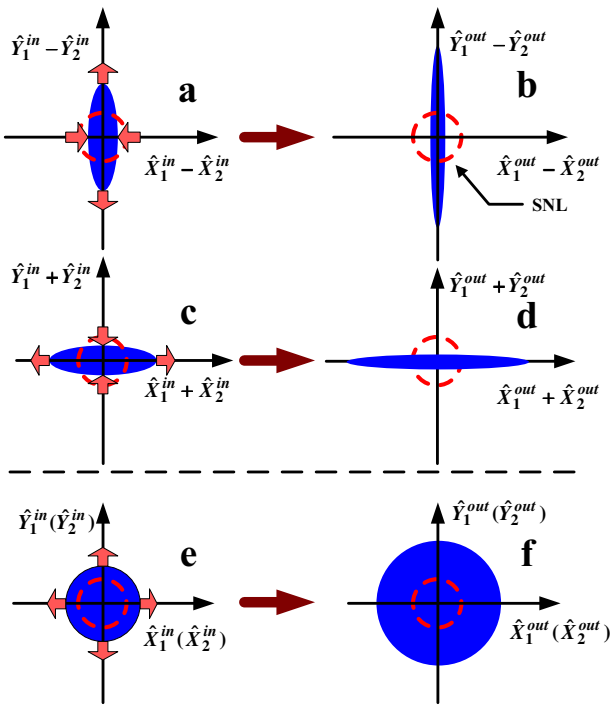

FIG. 5. (Color online) Schematics of the correlation and the quadrature components of the signal and idler fields in the phase space with an EPR entangled input beams for the NOPA operated at the state of amplification. (a) and (c) are the quantum correlations of the input signal and idler fields; (b) and (d) are the quantum correlations of the output signal and idler fields; (e) and (f) are the input and output quadrature components of the signal and idler fields.

$$\langle \delta^2(\hat{X}_1^o - \hat{X}_2^o)\rangle = \langle \delta^2(\hat{Y}_1^o + \hat{Y}_2^o)\rangle = 2e^{-2(r+r_0)},$$

$$\langle \delta^2(\hat{X}_1^o + \hat{X}_2^o)\rangle = \langle \delta^2(\hat{Y}_1^o - \hat{Y}_2^o)\rangle = 2e^{2(r+r_0)}. \quad (17)$$

Figure 5 shows the schematic of the correlation and the quadrature components of the signal and idler fields in the phase space with an EPR entangled input beams for the NOPA operated at the state of amplification. Obviously, the correlation degree of the input EPR entangled beams can be improved further by the nonlinear interaction r of the NOPA.

When the NOPA is operated at the state of deamplification, the quantum correlation variances between the two output modes are obtained from Eqs. (3),

$$\langle \delta^2(\hat{X}_1^o - \hat{X}_2^o)\rangle = \langle \delta^2(\hat{Y}_1^o + \hat{Y}_2^o)\rangle = 2e^{2(r-r_0)},$$

$$\langle \delta^2(\hat{X}_1^o + \hat{X}_2^o)\rangle = \langle \delta^2(\hat{Y}_1^o - \hat{Y}_2^o)\rangle = 2e^{-2(r-r_0)}. \quad (18)$$

It is obvious that if $r < r_0$, the input quadrature amplitude correlation and quadrature phase anticorrelation will be reduced by phase-sensitive NOPA. The quadrature amplitude correlation and quadrature phase anticorrelation will be changed into amplitude anticorrelation and quadrature phase correlation with the increase of r and $r > r_0$. When $r = r_0$, the signal and idler output fields become the vacuum states. Figure 6 shows the schematic of the correlation and the quadrature components of the signal and idler fields in the phase space with an EPR entangled input beams for the NOPA operated at the state of deamplification. From Eqs. (17) and (18), we find that the entangled degree of the output fields of the NOPA is different at the same parametric gain, which depends on the relative phase with the pump light.

III. OUTPUT SPECTRA OF QUANTUM CORRELATION OF NOPA INSIDE AN OPTICAL CAVITY

Now we consider the NOPA inside an optical cavity, which is pumped by harmonic wave of frequency $2\omega_0$ and injected by two subharmonic waves with frequency $\omega_1 + \omega_2 = \omega_p$ but orthogonal polarization. The mirror M2 is mounted on a piezoelectric transducer (PZT) to scan the NOPA cavity length. The output signal and idler beams combine with the local oscillator beam to be measured by the balanced homodyne detector, respectively, as shown in Fig. 7. The two intracavity subharmonic fields are described by $\hat{a}_1$ and $\hat{a}_2$ and the subharmonic input and output fields are denoted by $\hat{a}_1^{in}$, $\hat{a}_2^{in}$ and $\hat{a}_1^o$, $\hat{a}_2^o$, respectively. We suppose that there are identical losses for the intracavity fields $\hat{a}_1$ and $\hat{a}_2$. So we denote γ as the decay rate of the signal and idler modes due to transmission of the input-output coupler mirror M1 and γ_c due to all other intracavity losses, respectively. We denote by $\hat{c}_1$, $\hat{c}_2$ as the vacuum modes that are coupled into the signal and idler modes through the leakage loss γ_c.

The equations of motion for the intracavity signal and idler modes are as follows:

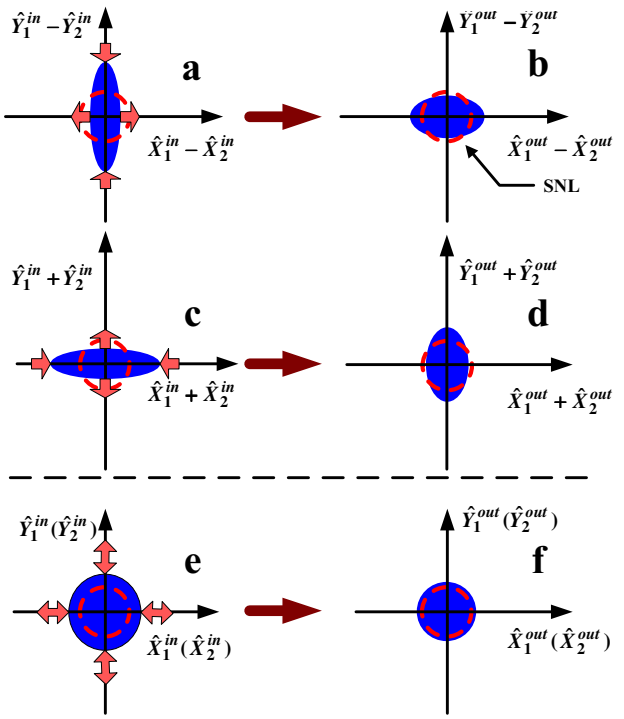

FIG. 6. (Color online) Schematics of the correlation and the quadrature components of the signal and idler fields in the phase space with an EPR entangled input beams for the NOPA operated at the state of deamplification. (a) and (c) are the quantum correlations of the input signal and idler fields; (b) and (d) are the quantum correlations of the output signal and idler fields; (e) and (f) are the input and output quadrature components of the signal and idler fields.

$$\frac{d\hat{a}_1}{dt} = -i\Delta\hat{a}_1 - (\gamma + \gamma_c)\hat{a}_1 + \kappa\hat{a}_2^\dagger \exp(i\theta_p) + \sqrt{2\gamma}\hat{a}_1^{in} + \sqrt{2\gamma_c}\hat{c}_1,$$

$$\frac{d\hat{a}_2}{dt} = -i\Delta\hat{a}_2 - (\gamma + \gamma_c)\hat{a}_2 + \kappa\hat{a}_1^\dagger \exp(i\theta_p) + \sqrt{2\gamma}\hat{a}_2^{in} + \sqrt{2\gamma_c}\hat{c}_2, \tag{19}$$

where θ_p is the phase of pump light and Δ is cavity detuning. Here we assume that the pump field is undepleted and described by a constant which is included in the coupling coefficient κ. We will take κ to be real without the loss of generality. Without loss of generality, the annihilation operators can be expressed in terms of a steady state and fluctuating component as $\hat{a}_i = \alpha_i + \delta\hat{a}_i$. By linearizing Eqs. (19), we obtain the fluctuation dynamic equations

$$\frac{d}{dt}\delta\hat{a}_1 = -i\Delta\delta\hat{a}_1 - (\gamma + \gamma_c)\delta\hat{a}_1 + \kappa\delta\hat{a}_2^\dagger \exp(i\theta_p) + \sqrt{2\gamma}\delta\hat{a}_1^{in} + \sqrt{2\gamma_c}\delta\hat{c}_1,$$

$$\frac{d}{dt}\delta\hat{a}_2 = -i\Delta\delta\hat{a}_2 - (\gamma + \gamma_c)\delta\hat{a}_2 + \kappa\delta\hat{a}_1^\dagger \exp(i\theta_p) + \sqrt{2\gamma}\delta\hat{a}_2^{in} + \sqrt{2\gamma_c}\delta\hat{c}_2. \tag{20}$$

In order to calculate the quantum correlation of the signal and idler modes, we define $\hat{d}_1 = \frac{1}{\sqrt{2}}(\hat{a}_1 + \hat{a}_2)$, $\hat{d}_2 = \frac{1}{\sqrt{2}}(\hat{a}_1 - \hat{a}_2)$ and their quadrature components are expressed by

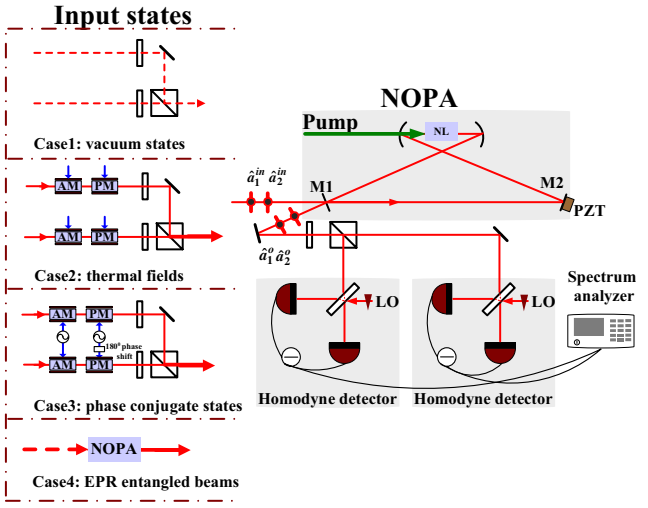

FIG. 7. (Color online) Schematics of the NOPA inside a cavity and the four different kinds of the input states. NL: type-II phase-matched nonlinear crystal; LO: local oscillator; M1: input-output coupler mirror; PM: phase modulator; AM: amplitude modulator; PZT: piezoelectric transducer; $\hat{a}_1^{in}$ and $\hat{a}_2^{in}$ are the injected signal and idler fields with degenerate frequency but orthogonal polarization; $\hat{a}_1^o$ and $\hat{a}_2^o$ are the output fields of the NOPA.

$$\hat{X}_{d_1} = \frac{1}{\sqrt{2}}(\hat{a}_1 + \hat{a}_2 + \hat{a}_1^\dagger + \hat{a}_2^\dagger) = (\hat{X}_{a_1} + \hat{X}_{a_2})/\sqrt{2},$$

$$\hat{Y}_{d_1} = \frac{1}{\sqrt{2}i}(\hat{a}_1 + \hat{a}_2 - \hat{a}_1^\dagger - \hat{a}_2^\dagger) = (\hat{Y}_{a_1} + \hat{Y}_{a_2})/\sqrt{2},$$

$$\hat{X}_{d_2} = \frac{1}{\sqrt{2}}(\hat{a}_1 - \hat{a}_2 + \hat{a}_1^\dagger - \hat{a}_2^\dagger) = (\hat{X}_{a_1} - \hat{X}_{a_2})/\sqrt{2},$$

$$\hat{Y}_{d_2} = \frac{1}{\sqrt{2}i}(\hat{a}_1 - \hat{a}_2 - \hat{a}_1^\dagger + \hat{a}_2^\dagger) = (\hat{Y}_{a_1} - \hat{Y}_{a_2})/\sqrt{2}. \tag{21}$$

Thus the equations of motion for the quadrature components fluctuations of the quantum correlation of the signal and idler mode can be obtained through Eqs. (20) and (21),

$$\frac{d}{dt}\delta\hat{X}_{d_1} = \Delta\delta\hat{Y}_{d_1} - (\gamma + \gamma_c)\delta\hat{X}_{d_1} + \kappa\hat{X}_{d_1}^{\theta_p} + \sqrt{2\gamma}\delta\hat{X}_{d_1}^{in} + \sqrt{2\gamma_c}\delta\hat{X}_{c_+},$$

$$\frac{d}{dt}\delta\hat{Y}_{d_1} = -\Delta\delta\hat{X}_{d_1} - (\gamma + \gamma_c)\delta\hat{Y}_{d_1} - \kappa\hat{Y}_{d_1}^{\theta_p} + \sqrt{2\gamma}\delta\hat{Y}_{d_1}^{in} + \sqrt{2\gamma_c}\delta\hat{Y}_{c_+},$$

$$\frac{d}{dt}\delta\hat{X}_{d_2} = \Delta\,\delta\hat{Y}_{d_2} - (\gamma+\gamma_c)\delta\hat{X}_{d_2} - \kappa\hat{X}^{\theta_p}_{d_2} + \sqrt{2\gamma}\delta\hat{X}^{in}_{d_2} + \sqrt{2\gamma_c}\delta\hat{X}_{c_-},$$

$$\frac{d}{dt}\delta\hat{Y}_{d_2} = -\Delta\,\delta\hat{X}_{d_2} - (\gamma+\gamma_c)\delta\hat{Y}_{d_2} + \kappa\hat{Y}^{\theta_p}_{d_2} + \sqrt{2\gamma}\delta\hat{Y}^{in}_{d_2} + \sqrt{2\gamma_c}\delta\hat{Y}_{c_-}, \tag{22}$$

where

$$\hat{X}^{in}_{d_1} = \frac{1}{\sqrt{2}}(\hat{a}^{in}_1 + \hat{a}^{in}_2 + \hat{a}^{in\dagger}_1 + \hat{a}^{in\dagger}_2),$$

$$\hat{Y}^{in}_{d_1} = \frac{1}{\sqrt{2}i}(\hat{a}^{in}_1 + \hat{a}^{in}_2 - \hat{a}^{in\dagger}_1 - \hat{a}^{in\dagger}_2),$$

$$\hat{X}^{\theta_p}_{d_1} = \frac{1}{\sqrt{2}}(\hat{a}_1 e^{-i\theta_p} + \hat{a}_2 e^{-i\theta_p} + \hat{a}^{\dagger}_1 e^{i\theta_p} + \hat{a}^{\dagger}_2 e^{i\theta_p}),$$

$$\hat{Y}^{\theta_p}_{d_1} = \frac{1}{\sqrt{2}i}(\hat{a}_1 e^{-i\theta_p} + \hat{a}_2 e^{-i\theta_p} - \hat{a}^{\dagger}_1 e^{i\theta_p} - \hat{a}^{\dagger}_2 e^{i\theta_p}),$$

$$\hat{X}_{c_+} = \frac{1}{\sqrt{2}}(\hat{c}_1 + \hat{c}_2 + \hat{c}^{\dagger}_1 + \hat{c}^{\dagger}_2),$$

$$\hat{Y}_{c_+} = \frac{1}{\sqrt{2}i}(\hat{c}_1 + \hat{c}_2 - \hat{c}^{\dagger}_1 - \hat{c}^{\dagger}_2),$$

$$\hat{X}^{in}_{d_2} = \frac{1}{\sqrt{2}}(\hat{a}^{in}_1 - \hat{a}^{in}_2 + \hat{a}^{in\dagger}_1 - \hat{a}^{in\dagger}_2),$$

$$\hat{Y}^{in}_{d_2} = \frac{1}{\sqrt{2}i}(\hat{a}^{in}_1 - \hat{a}^{in}_2 - \hat{a}^{in\dagger}_1 + \hat{a}^{in\dagger}_2),$$

$$\hat{X}^{\theta_p}_{d_2} = \frac{1}{\sqrt{2}}(\hat{a}_1 e^{-i\theta_p} - \hat{a}_2 e^{-i\theta_p} + \hat{a}^{\dagger}_1 e^{i\theta_p} - \hat{a}^{\dagger}_2 e^{i\theta_p}),$$

$$\hat{Y}^{\theta_p}_{d_2} = \frac{1}{\sqrt{2}i}(\hat{a}_1 e^{-i\theta_p} - \hat{a}_2 e^{-i\theta_p} - \hat{a}^{\dagger}_1 e^{i\theta_p} + \hat{a}^{\dagger}_2 e^{i\theta_p}),$$

$$\hat{X}_{c_-} = \frac{1}{\sqrt{2}}(\hat{c}_1 - \hat{c}_2 + \hat{c}^{\dagger}_1 - \hat{c}^{\dagger}_2),$$

$$\hat{Y}_{c_-} = \frac{1}{\sqrt{2}i}(\hat{c}_1 - \hat{c}_2 - \hat{c}^{\dagger}_1 + \hat{c}^{\dagger}_2). \tag{23}$$

Since the spectra of the quadrature variances of the output fields are measured and analyzed, we make the Fourier transformation $\hat{O}(\Omega) = \frac{1}{\sqrt{2\pi}}\int dt \hat{O}(t) e^{-i\Omega t}$ for the operators in Eqs. (22), with the commutation relation $[\hat{O}(\Omega), \hat{O}(\Omega')] = \delta(\Omega - \Omega')$. With the boundary condition $a^o_i(\Omega) = \sqrt{2\gamma}a_i(\Omega) - a^{in}_i(\Omega)$, the spectra of the quantum correlation of the output signal and idler mode in terms of the input fluctuation can be obtained

$$\begin{aligned}
\delta\hat{X}^o_{d_1}(\Omega) = \{&[(\gamma+\gamma_c \pm \kappa + i\Omega)(\gamma-\gamma_c \pm \kappa - i\Omega) \\
&- \Delta^2]\delta\hat{X}^{in}_{d_1}(\Omega) + 2\gamma\Delta\,\delta\hat{Y}^{in}_{d_1}(\Omega) \\
&+ 2\sqrt{\gamma\gamma_c}(\gamma+\gamma_c \pm \kappa + i\Omega)\delta\hat{X}_{c_+}(\Omega) \\
&+ 2\Delta\sqrt{\gamma\gamma_c}\delta\hat{Y}_{c_+}(\Omega)\} \\
&/[(\gamma+\gamma_c \pm \kappa + i\Omega)(\gamma+\gamma_c \mp \kappa + i\Omega) + \Delta^2], \\
\delta\hat{Y}^o_{d_1}(\Omega) = \{&[(\gamma+\gamma_c \mp \kappa + i\Omega)(\gamma-\gamma_c \mp \kappa - i\Omega) \\
&- \Delta^2]\delta\hat{Y}^{in}_{d_1}(\Omega) - 2\gamma\Delta\,\delta\hat{X}^{in}_{d_1}(\Omega) \\
&+ 2\sqrt{\gamma\gamma_c}(\gamma+\gamma_c \mp \kappa + i\Omega)\delta\hat{Y}_{c_+}(\Omega) \\
&- 2\Delta\sqrt{\gamma\gamma_c}\delta\hat{X}_{c_+}(\Omega)\} \\
&/[(\gamma+\gamma_c \pm \kappa + i\Omega)(\gamma+\gamma_c \mp \kappa + i\Omega) + \Delta^2], \\
\delta\hat{X}^o_{d_2}(\Omega) = \{&[(\gamma+\gamma_c \mp \kappa + i\Omega)(\gamma-\gamma_c \mp \kappa - i\Omega) \\
&- \Delta^2]\delta\hat{X}^{in}_{d_2}(\Omega) + 2\gamma\Delta\,\delta\hat{Y}^{in}_{d_2}(\Omega) \\
&+ 2\sqrt{\gamma\gamma_c}(\gamma+\gamma_c \mp \kappa + i\Omega)\delta\hat{X}_{c_-}(\Omega) \\
&+ 2\Delta\sqrt{\gamma\gamma_c}\delta\hat{Y}_{c_-}(\Omega)\} \\
&/[(\gamma+\gamma_c \pm \kappa + i\Omega)(\gamma+\gamma_c \mp \kappa + i\Omega) + \Delta^2], \\
\delta\hat{Y}^o_{d_2}(\Omega) = \{&[(\gamma+\gamma_c \pm \kappa + i\Omega)(\gamma-\gamma_c \pm \kappa - i\Omega) \\
&- \Delta^2]\delta\hat{Y}^{in}_{d_2}(\Omega) - 2\gamma\Delta\,\delta\hat{X}^{in}_{d_2}(\Omega) \\
&+ 2\sqrt{\gamma\gamma_c}(\gamma+\gamma_c \pm \kappa + i\Omega)\delta\hat{Y}_{c_-}(\Omega) \\
&- 2\Delta\sqrt{\gamma\gamma_c}\delta\hat{X}_{c_-}(\Omega)\} \\
&/[(\gamma+\gamma_c \pm \kappa + i\Omega)(\gamma+\gamma_c \mp \kappa + i\Omega) + \Delta^2],
\end{aligned} \tag{24}$$

where the plus and minus symbols at superscripts or subscripts correspond to the state of NOPA operated at amplification or deamplification, respectively. Subsequently, we can calculate the quantum correlation variance of the signal and idler beams

$$\begin{aligned}
\langle\delta^2\hat{X}^o_{d_1}(\Omega)\rangle = \{&[(\gamma \pm \kappa)^2 - \gamma_c^2 + \Omega^2 - \Delta^2]^2 + 4\gamma_c^2\Omega^2\} \\
&\times\langle\delta^2\hat{X}^{in}_{d_1}(\Omega)\rangle + 4\gamma^2\Delta^2\langle\delta^2\hat{Y}^{in}_{d_1}(\Omega)\rangle \\
&+ 4\Delta^2\gamma\gamma_c\langle\delta^2\hat{Y}_{c_+}(\Omega)\rangle + 4\gamma\gamma_c[(\gamma+\gamma_c \pm \kappa)^2 \\
&+ \Omega^2]\langle\delta^2\hat{X}_{c_+}(\Omega)\rangle/\{[(\gamma+\gamma_c)^2 + \Delta^2 - \Omega^2 - \kappa^2]^2 \\
&+ 4\Omega^2(\gamma+\gamma_c)^2\},
\end{aligned}$$

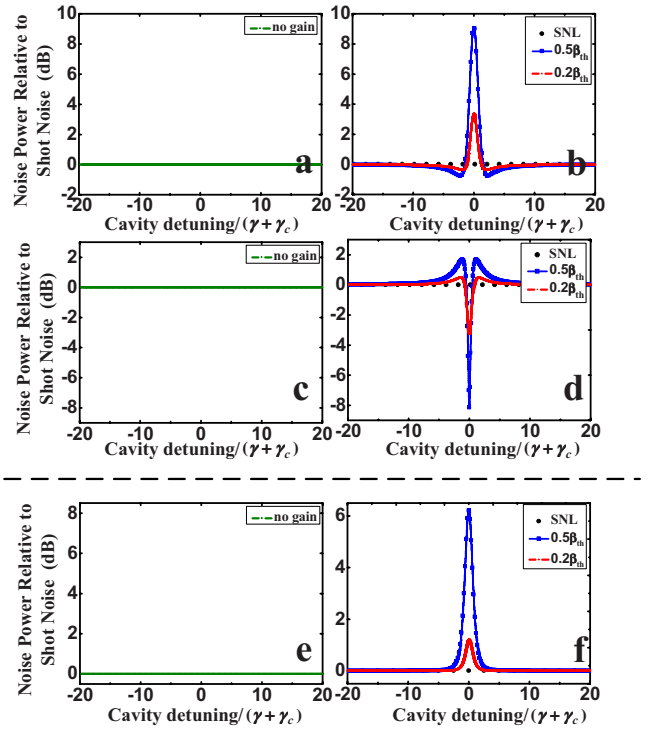

FIG. 8. (Color online) The noise power spectra of the quantum correlation and the quadrature components of the signal and idler fields of the NOPA injected with the vacuum state as a function of the cavity detuning for different pump powers. Quantum noise is analyzed at the sideband frequency of $\Omega=2$ MHz. (a) and (b) for the $(\hat{X}_1^o+\hat{X}_2^o)/\sqrt{2}$ [or $(\hat{Y}_1^o-\hat{Y}_2^o)/\sqrt{2}$]. (c) and (d) for $(\hat{X}_1^o-\hat{X}_2^o)/\sqrt{2}$ [or $(\hat{Y}_1^o+\hat{Y}_2^o)/\sqrt{2}$]. (e) and (f) for the amplitude or phase variances of the signal or idler modes of the NOPA.

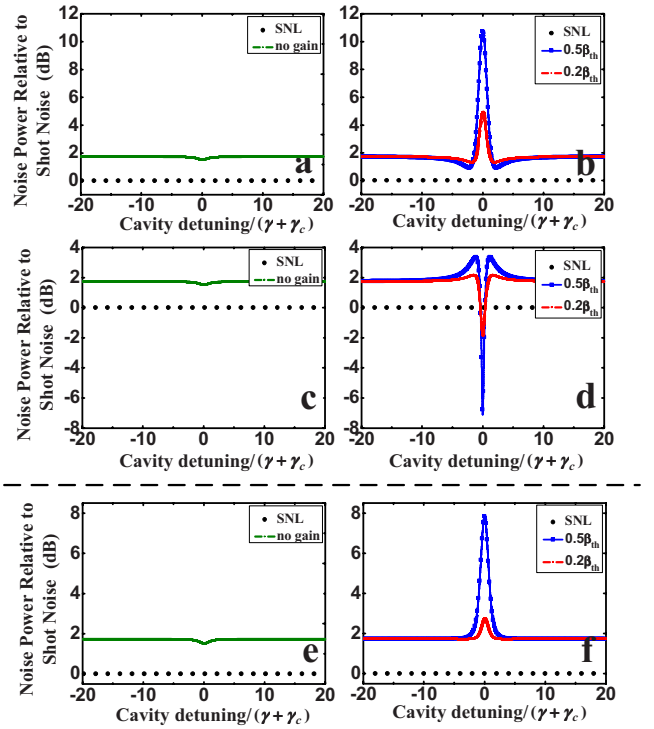

FIG. 9. (Color online) The noise power spectra of the quantum correlation and the quadrature components of the signal and idler fields of the NOPA injected with two uncorrelated thermal optical fields, as a function of the cavity detuning for different pump powers. All other parameters for the calculation are same as the Fig. 8. (a) and (b) for the $(\hat{X}_1^o+\hat{X}_2^o)/\sqrt{2}$ [or $(\hat{Y}_1^o-\hat{Y}_2^o)/\sqrt{2}$]. (c) and (d) for $(\hat{X}_1^o-\hat{X}_2^o)/\sqrt{2}$ [or $(\hat{Y}_1^o+\hat{Y}_2^o)/\sqrt{2}$]. (e) and (f) for the amplitude or phase variances of the signal or idler modes of the NOPA.

$$\langle\delta^2\hat{Y}_{d_1}^o(\Omega)\rangle = \{[(\gamma\mp\kappa)^2-\gamma_c^2+\Omega^2-\Delta^2]^2+4\gamma_c^2\Omega^2\}\times\langle\delta^2\hat{Y}_{d_1}^{in}(\Omega)\rangle+4\gamma^2\Delta^2\langle\delta^2\hat{X}_{d_1}^{in}(\Omega)\rangle+4\Delta^2\gamma\gamma_c\langle\delta^2\hat{X}_{c_+}(\Omega)\rangle+4\gamma\gamma_c[(\gamma+\gamma_c\mp\kappa)^2+\Omega^2]\langle\delta^2\hat{Y}_{c_+}(\Omega)\rangle/\{[(\gamma+\gamma_c)^2+\Delta^2-\Omega^2-\kappa^2]^2+4\Omega^2(\gamma+\gamma_c)^2\},$$

$$\langle\delta^2\hat{X}_{d_2}^o(\Omega)\rangle = \{[(\gamma\mp\kappa)^2-\gamma_c^2+\Omega^2-\Delta^2]^2+4\gamma_c^2\Omega^2\}\times\langle\delta^2\hat{X}_{d_2}^{in}(\Omega)\rangle+4\gamma^2\Delta^2\langle\delta^2\hat{Y}_{d_2}^{in}(\Omega)\rangle+4\Delta^2\gamma\gamma_c\langle\delta^2\hat{Y}_{c_-}(\Omega)\rangle+4\gamma\gamma_c[(\gamma+\gamma_c\mp\kappa)^2+\Omega^2]\langle\delta^2\hat{X}_{c_-}(\Omega)\rangle/\{[(\gamma+\gamma_c)^2+\Delta^2-\Omega^2-\kappa^2]^2+4\Omega^2(\gamma+\gamma_c)^2\},$$

$$\langle\delta^2\hat{Y}_{d_2}^o(\Omega)\rangle = \{[(\gamma\pm\kappa)^2-\gamma_c^2+\Omega^2-\Delta^2]^2+4\gamma_c^2\Omega^2\}\times\langle\delta^2\hat{Y}_{d_2}^{in}(\Omega)\rangle+4\gamma^2\Delta^2\langle\delta^2\hat{X}_{d_2}^{in}(\Omega)\rangle+4\Delta^2\gamma\gamma_c\langle\delta^2\hat{X}_{c_-}(\Omega)+4\gamma\gamma_c[(\gamma+\gamma_c\pm\kappa)^2+\Omega^2]\langle\delta^2\hat{Y}_{c_-}(\Omega)\rangle/\{[(\gamma+\gamma_c)^2+\Delta^2-\Omega^2-\kappa^2]^2+4\Omega^2(\gamma+\gamma_c)^2\}, \quad (25)$$

where $\langle\delta^2\hat{X}_{c_+}(\Omega)\rangle=\langle\delta^2\hat{Y}_{c_+}(\Omega)\rangle=\langle\delta^2\hat{X}_{c_-}(\Omega)\rangle=\langle\delta^2\hat{Y}_{c_-}(\Omega)\rangle=1$ since they are vacuum input fields. The variances of the signal and idler output fields are expressed by

$$\langle\delta^2\hat{X}_{a_1}^o(\Omega)\rangle=\langle\delta^2\hat{X}_{a_2}^o(\Omega)\rangle=\frac{\langle\delta^2\hat{X}_{d_1}^o(\Omega)\rangle+\langle\delta^2\hat{X}_{d_2}^o(\Omega)\rangle}{2},$$

$$\langle\delta^2\hat{Y}_{a_1}^o(\Omega)\rangle=\langle\delta^2\hat{Y}_{a_2}^o(\Omega)\rangle=\frac{\langle\delta^2\hat{Y}_{d_1}^o(\Omega)\rangle+\langle\delta^2\hat{Y}_{d_2}^o(\Omega)\rangle}{2}. \quad (26)$$

Case 1. We first study the NOPA by injecting vacuum states at the signal and idler fields. When the pump field is blocked, the parametric process is not active and the quantum correlation variances of the output modes correspond to the shot-noise limit (SNL) as shown in Figs. 8(a) and 8(c). When the pump field is injected into the NOPA, we fix the phase of the pump field $\theta_p=0$ and select the suitable phases of local oscillators to measure the quadratures of the signal and idler fields, respectively. Let us examine the quantum

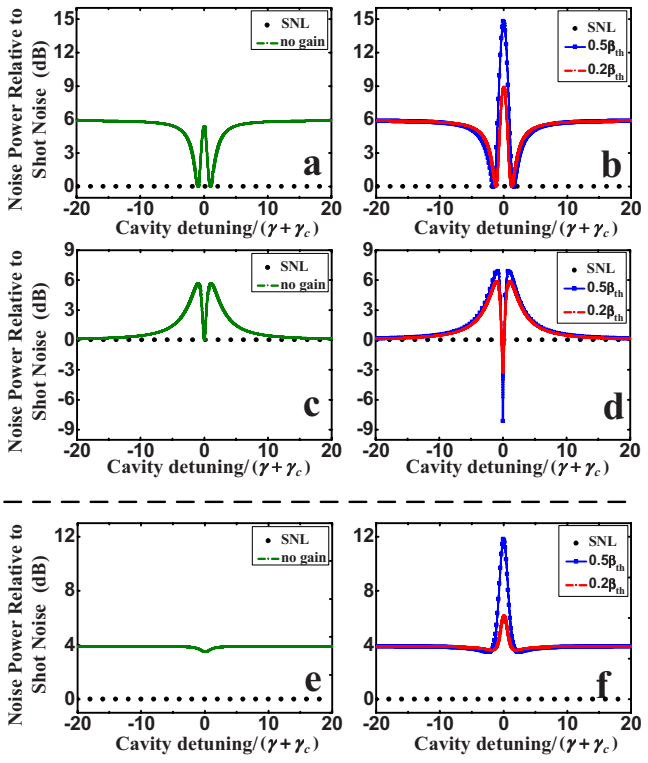

FIG. 10. (Color online) The noise power spectra of the quantum correlation and the quadrature components of the signal and idler fields of the NOPA injected with a pair of phase-conjugate states as a function of the cavity detuning for different pump powers. The NOPA is operated at the state of amplification. All other parameters for the calculation are same as the Fig. 8. (a) and (b) for the $(\hat{X}_1^o+\hat{X}_2^o)/\sqrt{2}$ [or $(\hat{Y}_1^o-\hat{Y}_2^o)/\sqrt{2}$]. (c) and (d) for $(\hat{X}_1^o-\hat{X}_2^o)/\sqrt{2}$ [or $(\hat{Y}_1^o+\hat{Y}_2^o)/\sqrt{2}$]. (e) and (f) for the amplitude or phase variances of the signal or idler modes of the NOPA.

correlation variance of the signal and idler beams at $\Omega=2$ MHz as a function of the cavity detuning. All the parameters are chosen in units of the total decay rate $\gamma+\gamma_c$ of the cavity. Figures 8(b), 8(d), and 8(f) show the noise power spectra of the quantum correlation and the quadrature components of the signal and idler output fields with the input vacuum input state at the different pump levels $0.2\beta_{th}$ and $0.5\beta_{th}$, where $\beta_{th}=(\gamma+\gamma_c)/g$ is the OPO threshold amplitude. As the pump power is increased, the degrees of the amplitude correlation and the phase anticorrelation $(\hat{X}_1^o-\hat{X}_2^o$ and $\hat{Y}_1^o+\hat{Y}_2^o)$ are greatly increased at the resonance, while the quantum correlation variances of the $\hat{X}_1^o+\hat{X}_2^o$ and $\hat{Y}_1^o-\hat{Y}_2^o$ become much noisier, which is a requirement of Heisenberg uncertainty relation. When we check the signal (or idler) output fields, the conjugate pairs of quadratures are all higher than SNL, which correspond to the thermal state. As one can see, the shoulders appear peak (dip) for both the amplitude correlation [or the phase anticorrelation, Fig. 8(d)] and the amplitude anticorrelation [or the phase correlation, Fig. 8(b)] spectra just outside the resonant, which indicate that small deamplification can occur when the cavity is detuned from the resonance even for the amplified operation at resonance.

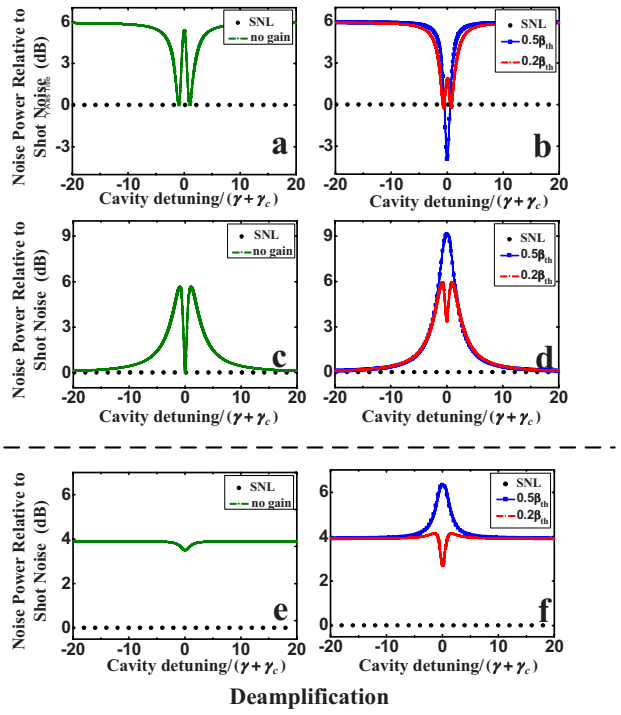

FIG. 11. (Color online) The noise power spectra of the quantum correlation and the quadrature components of the signal and idler fields of the NOPA injected with a pair of phase-conjugate states as a function of the cavity detuning for different pump powers. The NOPA is operated at the state of deamplification. All other parameters for the calculation are same as the Fig. 8. (a) and (b) for the $(\hat{X}_1^o+\hat{X}_2^o)/\sqrt{2}$ [or $(\hat{Y}_1^o-\hat{Y}_2^o)/\sqrt{2}$]. (c) and (d) for $(\hat{X}_1^o-\hat{X}_2^o)/\sqrt{2}$ [or $(\hat{Y}_1^o+\hat{Y}_2^o)/\sqrt{2}$]. (e) and (f) for the amplitude or phase variances of the signal or idler modes of the NOPA.

The spectra at the detuning far from the cavity resonance correspond to the noise of input fields because the input fields do not interact with the pump field by nonlinear crystal.

Case 2. Now consider the two uncorrelated thermal fields as the input signal and idler fields. The thermal states can be generated at sidebands of bright laser modes. These sidebands, originally in the vacuum state, are excited by the use of amplitude and phase modulators driven by four independent and uncorrelated signal generators as shown Fig. 7. By fixing an arbitrary phase of the pump light and selecting the proper phases of local oscillators, the noise power spectra of the quantum correlation and quadrature components of the output signal and idler fields of the NOPA are shown in Fig. 9. Figures 9(a) and 9(c) show the quantum-correlated variances without pump beam, which all are above the SNL. When the pump beam is turned on with different pump powers $0.2\beta_{th}$ and $0.5\beta_{th}$, the quantum correlation variances dependent of cavity detuning are shown in Figs. 9(b) and 9(d). It is shown that the shape of the spectra of quantum correlation variances with input thermal fields is similar as the input vacuum states. The difference exists in the background level above the SNL for input thermal states.

Case 3. Now let us concentrate on the NOPA injected with a pair of phase-conjugate states as the input signal and idler light. The phase-conjugate states can be generated by the use

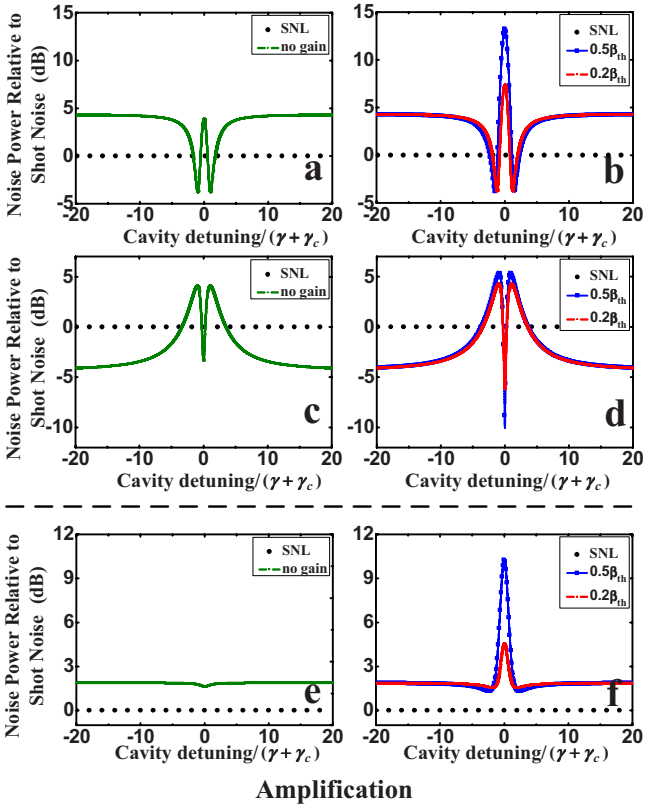

FIG. 12. (Color online) The noise power spectra of the quantum correlation and the quadrature components of the signal and idler fields of the NOPA injected with a pair of EPR entangled states, as a function of the cavity detuning for different pump powers, when the NOPA is operated at the state of amplification. All other parameters for the calculation are same as the Fig. 8. (a) and (b) for the $(\hat{X}_1^o+\hat{X}_2^o)/\sqrt{2}$ [or $(\hat{Y}_1^o-\hat{Y}_2^o)/\sqrt{2}$]. (c) and (d) for $(\hat{X}_1^o-\hat{X}_2^o)/\sqrt{2}$ [or $(\hat{Y}_1^o+\hat{Y}_2^o)/\sqrt{2}$]. (e) and (f) for the amplitude or phase variances of the signal or idler modes of the NOPA.

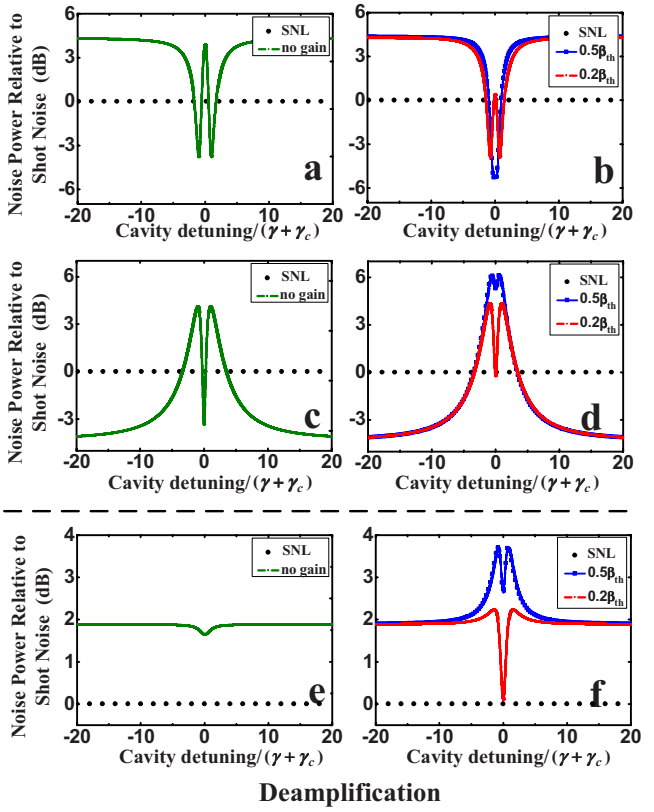

FIG. 13. (Color online) The noise power spectra of the quantum correlation and the quadrature components of the signal and idler fields of the NOPA injected with a pair of EPR entangled states, as a function of the cavity detuning for different pump powers, when the NOPA is operated at the state of deamplification. All other parameters for the calculation are same as the Fig. 8. (a) and (b) for the $(\hat{X}_1^o+\hat{X}_2^o)/\sqrt{2}$ [or $(\hat{Y}_1^o-\hat{Y}_2^o)/\sqrt{2}$]. (c) and (d) for $(\hat{X}_1^o-\hat{X}_2^o)/\sqrt{2}$ [or $(\hat{Y}_1^o+\hat{Y}_2^o)/\sqrt{2}$]. (e) and (f) for the amplitude or phase variances of the signal or idler modes of the NOPA.

of amplitude and phase modulators driven by two independent and uncorrelated signal generators as shown Fig. 7. One of the phase modulators was driven by a π out of phase with respect to the other one using one of the signal generators to ensure the production of phase-conjugate beams. In contrast, the amplitude modulators are driven in phase by another signal generator. When the pump beam for the NOPA is blocked, the spectra of the quantum correlation variances and the individual quadrature components are shown in Figs. 10(a), 10(c), 10(e), 11(a), 11(c), and 11(e). These spectral shapes are induced by the absorption and dispersion properties of the "empty cavity" [19]. These figures are used as a reference level to examine the effect of the NOPA inside cavity on the input states.

First, we consider the NOPA operated at the state of amplification with pump powers of $0.2\beta_{th}$ and $0.5\beta_{th}$, respectively [Figs. 10(b), 10(d), and 10(f)]. Figure 10(d) shows the degree of the amplitude correlation and the phase anticorrelation is greatly increased at the resonance due to the parametric process. Correspondingly, the variances of the amplitude anticorrelation and the phase correlation become noisier than the input fields as shown in Fig. 10(b). The quantum fluctuations of the conjugate pair of quadratures of the output signal (or idler) fields are all higher than that of the input fields [Fig. 10(f)]. The shoulders in the spectra are also changed by the parametric process. When the NOPA is operated at the state of deamplification, the spectra of the quantum correlation variances and the individual quadrature components are shown in Figs. 11(b), 11(d), and 11(f). The amplitude anticorrelation and the phase correlation are changed from very noisy initially to possess nonlocal correlation at the resonance with the increase of the parametric gain [Fig. 11(b)]. However, the amplitude correlation and the phase anticorrelation will be changed from nonlocal correlation to very noisy [Fig. 11(d)]. The quantum fluctuations of the conjugate pair of quadratures of the signal (or idler) output fields will first decrease and reach the minimum value (above the SNL), then increase with the increment of the parametric gain [Fig. 11(f)]. From the above analysis, we find that the degree of the correlation of the output modes of the NOPA injected with a pair of phase-conjugate states depends on the phase of the pump light.

Case 4. Let us now examine the situation with a pair of EPR beams possessing the feature of quadrature amplitude

correlation and quadrature phase anticorrelation, i.e., $\langle \delta^2(\hat{X}_1^{in} - \hat{X}_2^{in})\rangle = \langle \delta^2(\hat{Y}_1^{in} + \hat{Y}_2^{in})\rangle = 2e^{-2r_0}$ and $\langle \delta^2(\hat{X}_1^{in} + \hat{X}_2^{in})\rangle = \langle \delta^2(\hat{Y}_1^{in} - \hat{Y}_2^{in})\rangle = 2e^{2r_0}$, as the input signal and idler light. Figures 12(a), 12(c), 12(e), 13(a), 13(c), and 13(e) show the spectra of the quantum correlation variances and the individual quadrature components of the output signal and idler fields without pump light. These spectral shapes are induced by the absorption and dispersion properties of the "empty cavity" [19], which are similar as that for the input phase-conjugate states.

First, let us look at the quantum correlation variance of the output signal and idler modes by setting the pump phase $\theta_p = 0$ (the NOPA is operated at the state of amplification). The quadrature amplitude correlation and quadrature phase anticorrelation of output signal and idler fields are shown in Fig. 12(d) with the different pump powers $0.2\beta_{th}$ and $0.5\beta_{th}$. We can see that the degree of the quantum correlation at the resonance can be improved by the NOPA. This indicates a further increase of the quantum correlation by the NOPA inside a cavity. While fixing the pump phase and choosing the proper phase of the local oscillators, the quantum correlation variances of $\hat{X}_1^o + \hat{X}_2^o$ (or $\hat{Y}_1^o - \hat{Y}_2^o$) are shown in Fig. 12(b). The central peak is significantly amplified, which corresponds to the degree of its conjugate correlations (the quadrature amplitude correlation and quadrature phase anticorrelation) are improved at the resonance as shown in Fig. 12(d). The quantum fluctuations of the conjugate pair of quadratures of the signal (or idler) output fields will increase at the resonance and decrease a little at the two detuning shoulders with the increment of the parametric gain [Fig. 12(f)]. When the NOPA is operated at the state of deamplification, the spectra of the quantum correlation variances and the individual quadrature components are shown in Figs. 13(b), 13(d), and 13(f), which are similar as that for the input phase-conjugate states. It is important that investigating the quantum correlation variances and the individual quadrature components should be compared to SNL.

IV. CONCLUSION

In summary, we have studied theoretically quantum interferences between different kinds of input quantized fields and generated quantum fields from the NOPA operated inside the cavity. Spectral line shapes due to quantum interferences are investigated by scanning the length of the NOPA cavity. The results indicate that the NOPA inside an optical cavity can be used as an amplification device for the degree of the correlation when the relative phase between the pump beam and the injected EPR entangled beams is chosen properly. This manipulation of quantum fluctuations by a phase-sensitive optical amplifier is essential in quantum information processing and quantum networking [20].

ACKNOWLEDGMENTS

This research was supported in part by NSFC for Distinguished Young Scholars (Grant No. 10725416), National Basic Research Program of China (Grant No. 2006CB921101), NSFC Project for Excellent Research Team (Grant No. 60821004), and NSFC (Grants No. 60678029 and No. 60736040).

[1] Z. Y. Ou, S. F. Pereira, H. J. Kimble, and K. C. Peng, Phys. Rev. Lett. **68**, 3663 (1992); Y. Zhang, H. Wang, X. Li, J. Jing, C. Xie, and K. Peng, Phys. Rev. A **62**, 023813 (2000); V. D'Auria *et al.*, Phys. Rev. Lett. **102**, 020502 (2009).

[2] C. Fabre, E. Giacobino, A. Heidmann, and S. Reynaud, J. Phys. **50**, 1209 (1989); J. Laurat, L. Longchambon, and C. Fabre, Opt. Lett. **30**, 1177 (2005); A. S. Villar *et al.*, Phys. Rev. Lett. **95**, 243603 (2005); X. Su, A. Tan, X. Jia, Q. Pan, C. Xie, and K. Peng, Opt. Lett. **31**, 1133 (2006); J. Jing, S. Feng, R. Bloomer, and O. Pfister, Phys. Rev. A **74**, 041804(R) (2006).

[3] X. Li *et al.*, Phys. Rev. Lett. **88**, 047904 (2002).

[4] X. Jia, X. Su, Q. Pan, J. Gao, C. Xie, and K. Peng, Phys. Rev. Lett. **93**, 250503 (2004).

[5] A. Lamas-Linares, C. Simon, J. C. Howell, and D. Bouwmeester, Science **296**, 712 (2002); F. De Martini, D. Pelliccia, and F. Sciarrino, Phys. Rev. Lett. **92**, 067901 (2004); G. M. D'Ariano, F. De Martini, and M. F. Sacchi, *ibid.* **86**, 914 (2001).

[6] R. Bruckmeier, K. Schneider, S. Schiller, and J. Mlynek, Phys. Rev. Lett. **78**, 1243 (1997).

[7] T. C. Ralph, Opt. Lett. **24**, 348 (1999).

[8] H. Ma, C. Ye, D. Wei, and J. Zhang, Phys. Rev. Lett. **95**, 233601 (2005).

[9] C. Ye and J. Zhang, Phys. Rev. A **73**, 023818 (2006); Opt. Lett. **33**, 1911 (2008).

[10] G. S. Agarwal, Phys. Rev. Lett. **97**, 023601 (2006).

[11] J. Zhang *et al.*, Phys. Rev. Lett. **101**, 233602 (2008).

[12] R. Simon, Phys. Rev. Lett. **84**, 2726 (2000).

[13] L.-M. Duan, G. Giedke, J. I. Cirac, and P. Zoller, Phys. Rev. Lett. **84**, 2722 (2000).

[14] N. J. Cerf and S. Iblisdir, Phys. Rev. A **64**, 032307 (2001).

[15] N. J. Cerf and S. Iblisdir, Phys. Rev. Lett. **87**, 247903 (2001).

[16] H. Chen and J. Zhang, Phys. Rev. A **75**, 022306 (2007).

[17] M. Sabuncu, U. L. Andersen, and G. Leuchs, Phys. Rev. Lett. **98**, 170503 (2007).

[18] J. Niset *et al.*, Phys. Rev. Lett. **98**, 260404 (2007).

[19] M. D. Levenson, R. M. Shelby, and S. H. Perlmutter, Opt. Lett. **10**, 514 (1985); P. Galatola, L. A. Lugiato, M. G. Porreca, P. Tombesi, and G. Leuchs, Opt. Commun. **85**, 95 (1991); J. Zhang, T. Zhang, K. Zhang, C. Xie, and K. Peng, J. Opt. Soc. Am. B **17**, 1920 (2000); A. Zavatta, F. Marin, and G. Giacomelli, Phys. Rev. A **66**, 043805 (2002).

[20] S. L. Braunstein and A. K. Pati, *Quantum Information with Continuous Variables* (Kluwer Academic, Dordrecht, 2003); S. L. Braunstein and P. van Loock, Rev. Mod. Phys. **77**, 513 (2005).